Dependence of Activity and Stability of Germanium Nitride Powder for Photocatalytic Overall Water Splitting on Structural Properties

Kazuhiko Maeda,[†,‡] Nobuo Saito,[§] Yasunobu Inoue,[§] and Kazunari Domen*[,†]

Department of Chemical System Engineering, The University of Tokyo, 7-3-1 Hongo, Bunkyo-ku, Tokyo 113-8656, Japan and Department of Chemistry, Nagaoka University of Technology, Nagaoka 940-2188, Japan

Received April 10, 2007. Revised Manuscript Received May 26, 2007

Germanium nitride (Ge_3N_4) powder prepared by thermal ammonolysis of GeO_2 is examined as a photocatalyst for overall water splitting. Nitridation of GeO_2 under a flow of NH_3 at temperatures higher than 1123 K for 10 h results in production of either a single phase of β-Ge_3N_4 or a mixture of elemental Ge, α-Ge_3N_4, and β-Ge_3N_4, depending on the nitridation conditions. β-Ge_3N_4 exhibits activity for the stoichiometric decomposition of pure water into H_2 and O_2 under ultraviolet (UV) irradiation ($\lambda > 200$ nm) when loaded with nanoparticulate RuO_2 as a cocatalyst. Improving the crystallinity of the β-Ge_3N_4 catalyst results in greater activity for overall water splitting and markedly reduced N_2 release due to self-decomposition by photogenerated holes.

1. Introduction

Germanium nitride (Ge_3N_4) has attracted attention as a functional material with a range of useful properties, including high hardness[1] and dielectric[2] and photocatalytic[3] properties. Ge_3N_4 is a well-known polymorphic compound, of which Si_3N_4 is another typical example, exhibiting α, β, γ, and δ phases with various crystal structures.[4−6] It is believed that the α polymorph is a high-temperature phase that is metastable under ambient conditions, while the β phase is a thermodynamically stable form at low temperatures. McMillan et al. reported that γ-Ge_3N_4 can be obtained by heating the α or β form at 1000−1500 K under high pressure or reacting elemental Ge with N_2 under high-temperature and -pressure conditions.[6] It has also been claimed that δ-Ge_3N_4 can be obtained by high-pressure treatment (24 GPa) of the β form using a diamond anvil cell.[6]

Particulate metal nitrides including Ge_3N_4 can be readily obtained by thermal ammonolysis of the corresponding precursor, and the physicochemical properties of metal nitrides are controllable by appropriate adjustment of the preparation conditions.[7−17] Although several researchers have carried out high-pressure synthesis of Ge_3N_4 polymorphs using commercial Ge_3N_4 powder as a starting material,[4−6] research on the preparation of Ge_3N_4 powder by thermal ammonolysis at atmospheric pressure remains relatively rare despite the simplicity of such an approach.[7] Johnson presented a report on the preparation of Ge_3N_4 powder by nitriding Ge or GeO_2 powder under NH_3 flow.[7] However, systematic study on the relationship between the preparation conditions and the physicochemical properties of the products has yet to be undertaken. In general, the functionality of a given material is strongly dependent on the structural characteristics.[3b,15,18−23] Therefore, investigating the relationship between the functionality and structural char-

* To whom corresponding author should be addressed. Phone: +81-3-5841-1148. Fax: +81-3-5841-8838. E-mail: domen@chemsys.t.u-tokyo.ac.jp.
† The University of Tokyo.
‡ Research Fellow of the Japan Society for the Promotion of Science (JSPS).
§ Nagaoka University of Technology.

(1) Gao, F.; Xu, R.; Liu, K. *Phys. Rev. B* **2005**, *71*, 052103.
(2) (a) Yashiro, T. *J. Electrochem. Soc.* **1972**, *119*, 780. (b) Maeda, T.; Yasuda, T.; Nishizawa, M.; Miyata, N.; Morita, Y.; Takagi, S. *Appl. Phys. Lett.* **2004**, *85*, 3181. (c) Wang, S. J.; Chai, J. W.; Pan, J. S.; Huan, A. C. H. *Appl. Phys. Lett.* **2006**, *89*, 022105.
(3) (a) Sato, J.; Saito, N.; Yamada, Y.; Maeda, K.; Takata, T.; Kondo, J. N.; Hara, M.; Kobayashi, H.; Domen, K.; Inoue, Y. *J. Am. Chem. Soc.* **2005**, *127*, 4150. (b) Lee, Y.; Watanabe, T.; Takata, T.; Hara, M.; Yoshimura, M.; Domen, K. *J. Phys. Chem. B* **2006**, *110*, 17563. (c) Maeda, K.; Saito, N.; Lu, D.; Inoue, Y.; Domen, K. *J. Phys. Chem. C* **2007**, *111*, 4749.
(4) Dong, J.; Sankey, O. F.; Deb, S. K.; Wolf, G.; McMillan, P. F. *Phys. Rev. B* **2000**, *61*, 11979.
(5) Deb, S. K.; Dong, J.; Hubertc, H.; McMillana, P. F.; Sankey, O. F. *Solid State Commun.* **2000**, *114*, 137.
(6) Soignard, E.; McMillan, P. F.; Hejny, C.; Leinenweberd, K. *J. Solid State Chem.* **2004**, *177*, 299.
(7) Johnson, W. C. *J. Am. Chem. Soc.* **1930**, *52*, 5160.
(8) Brown, G. M.; Maya, L. *J. Am. Ceram. Soc.* **1988**, *71*, 78.
(9) Houmes, J. D.; Bem, D. S.; zur Loye, H.-C. *Mater. Res. Soc. Symp. Proc.* **1994**, *327*, 153.
(10) Tessier, F.; Marchand, R. *J. Alloys Compd.* **1997**, *262−263*, 410.
(11) Tessier, F.; Marchand, R.; Laurent, Y. *J. Eur. Ceram. Soc.* **1997**, *17*, 1825.
(12) Marchand, R.; Tessier, F.; DiSalvo, F. J. *J. Mater. Chem.* **1999**, *9*, 297.
(13) Schwenzer, B.; Loeffler, L.; Seshadri, R.; Keller, S.; Lange, F. F.; DenBaars, S. P.; Mishra, U. K. *J. Mater. Chem.* **2004**, *14*, 637.
(14) Niewa, R.; DiSalvo, F. J. *Chem. Mater.* **1998**, *10*, 2733.
(15) Hitoki, G.; Ishikawa, A.; Takata, T.; Kondo, J. N.; Hara, M.; Domen, K. *Chem. Lett.* **2002**, *31*, 736.
(16) Zhang, Q.; Gao, L. *Langmuir* **2004**, *20*, 9821.
(17) Schwenzer, B.; Hu, J.; Seshadri, R.; Keller, S.; DenBaars, S. P.; Mishra, U. K. *Chem. Mater.* **2004**, *16*, 5088.
(18) (a) Domen, K.; Naito, S.; Soma, M.; Onishi, T.; Tamaru, K. *J. Chem. Soc., Chem. Commun.* **1980**, 543. (b) Domen, K.; Naito, S.; Onishi, T.; Tamaru, K. *Chem. Phys. Lett.* **1982**, *92*, 433. (c) Kudo, A.; Tanaka, A.; Domen, K.; Onishi, T. *J. Catal.* **1988**, *111*, 296.
(19) (a) Domen, K.; Kudo, A.; Shinozaki, A.; Tanaka, A.; Maruya, K.; Onishi, T. *J. Chem. Soc., Chem. Commun.* **1986**, 356. (b) Kudo, A.; Tanaka, A.; Domen, K.; Maruya, K.; Aika, K.; Onishi, T. *J. Catal.* **1988**, *111*, 67. (c) Kudo, A.; Sayama, K.; Tanaka, A.; Asakura, A.; Domen, K.; Maruya, K.; Aika, K.; Onishi, T. *J. Catal.* **1989**, *111*, 337.

10.1021/cm0709828 CCC: $37.00 © 2007 American Chemical Society
Published on Web 07/17/2007

acteristics of a material is of interest and expected to provide useful information.

Our group has studied Ge_3N_4 as a non-oxide photocatalyst for overall water splitting.[3] Although much research on active photocatalysts for overall water splitting has been conducted over the past three decades, attention has been devoted almost exclusively to certain metal oxides such as $SrTiO_3$,[18] $K_4Nb_6O_{17}$,[19] $NaTaO_3$,[20] $NaInO_2$,[21] $M_2Sb_2O_7$ (M = Ca, Sr),[22] and Zn_2GeO_4.[23] Ge_3N_4 was presented as the first successful example of a non-oxide photocatalyst that can achieve the stoichiometric decomposition of pure water into H_2 and O_2 when modified with nanoparticulate RuO_2 as a cocatalyst for H_2 evolution.[3a] Since this discovery, the photocatalytic properties and effects of post-treatment to enhance the activity of Ge_3N_4 have been examined in detail.[3b,c] However, the relationship between the structural characteristics and the photocatalytic performance of Ge_3N_4 has yet to be investigated in detail.

In this study, Ge_3N_4 is prepared from GeO_2 powder by thermal ammonolysis and the obtained products are examined as a photocatalyst for overall water splitting. The relationship between the physicochemical properties and the catalytic performance of the material is discussed on the basis of the results of structural analyses.

2. Experimental Section

2.1. Preparation of Ge_3N_4. Ge_3N_4 powder was prepared by heating GeO_2 (Kanto Chemicals, 99.99%) powder (ca. 2 g) at temperatures of 1073−1223 K under NH_3 flow (100 mL/min). The nitridation reactor was connected directly to a silicon oil bubbler, and the effluent gas with entrained water generated during nitridation was passed into the bubbler at 393 K to prevent contamination by water and O_2 in air. After 5−20 h of nitridation, the sample was cooled to room temperature under NH_3 flow and then ground into a powder.

2.2. Modification with RuO_2 Nanoparticles. Nanoparticulate RuO_2 was loaded as a cocatalyst according to the method described previously.[3,11,21−23] Briefly, the as-prepared material was immersed in a tetrahydrofuran (THF) solution containing dissolved $Ru_3(CO)_{12}$ (Aldrich Chemical Co., 99%) followed by stirring at 333 K for 4 h. The solution was then dried under reduced pressure by heating in air at 373 K for 1 h to remove THF. The resulting powder was finally heated in air at 673 K for 5 h to convert the Ru species to RuO_2 nanoparticles. Nanoparticulate RuO_2 impregnated in this way was loaded at a rate of 1 wt %.

2.3. Characterization of Catalysts. The prepared samples were studied by powder X-ray diffraction (XRD; RINT-Ultima-III, Rigaku; Cu Kα), scanning electron microscopy (SEM; S-4700, Hitachi), and UV−vis diffuse reflectance spectroscopy (DRS; V-560, Jasco). Diffuse reflection spectra were converted from reflectance to absorbance by the Kubelka−Munk method, and each spectrum was normalized with respect to the Kubelka−Munk function at 250 nm. The Brunauer−Emmett−Teller (BET) surface area was measured using a BELSORP-mini instrument (BEL Japan) at liquid nitrogen temperature.

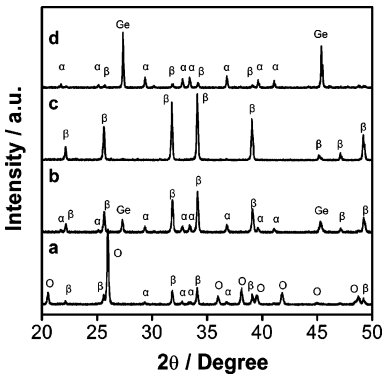

Figure 1. Powder XRD patterns of samples obtained by nitriding GeO_2 under NH_3 flow for 10 h at (a) 1073, (b) 1123, (c) 1173, and (d) 1223 K. α, *β*, Ge, and O denote diffractions assigned to α-Ge_3N_4, *β*-Ge_3N_4, elemental Ge, and GeO_2.

2.4. Photocatalytic Reactions. Reactions were typically carried out in a quartz inner-irradiation-type reaction vessel connected to a glass closed gas circulation system. A 0.3 g sample of the cocatalyst-loaded catalyst was dispersed in distilled water (360 mL), and the solution was evacuated several times to remove air completely. The cell was then irradiated at wavelengths longer than 200 nm using a 450 W high-pressure Hg lamp (UM-452, Ushio). The temperature of the reactant solution was maintained at room temperature by a flow of cooling water during the reaction. The evolved gases were analyzed by gas chromatography.

3. Results and Discussion

3.1. Thermal Ammonolysis of GeO_2. Figure 1 shows the XRD patterns of samples prepared by nitriding GeO_2 at temperatures in the range 1073−1223 K for 10 h. The sample nitrided at 1073 K consisted mainly of GeO_2 derived from the starting material with a small mixing of α- and *β*-Ge_3N_4 phase. At 1123 K, the diffraction peaks assigned to GeO_2 disappeared completely, and the obtained sample was a mixture of Ge and α- and *β*-Ge_3N_4. This result indicates that NH_3 gas at 1123 K under the present experimental conditions is sufficient to achieve complete transformation of GeO_2. A single phase of *β*-Ge_3N_4 was obtained at 1173 K, suggesting that the phase transition from α- to *β*-Ge_3N_4 takes place between 1123 and 1173 K under the present nitridation conditions. Nitridation at 1223 K resulted in production of elemental Ge and α-Ge_3N_4 with a small mixing of *β*-Ge_3N_4 phase attributed to decomposition of Ge_3N_4.[24] Johnson claimed that at 1173−1273 K GeO_2 reduces (by H_2 derived from NH_3) to Ge, Ge reacts with NH_3 to form Ge_3N_4, and Ge_3N_4 decomposes into elemental Ge and N_2.[7] The changes in the XRD patterns with increasing temperature from 1123 to 1223 K are consistent with Johnson's report. However, the nitridation products observed in the present study after heating at 1073 K were found to consist of a small amount of α- and *β*-Ge_3N_4 without appearance of the Ge phase. Therefore, it seems that Ge_3N_4 is obtained directly from GeO_2 by substituting N^{3-} for O^{2-} anions while maintaining the

(20) (a) Kato, H.; Kudo, A. *Chem. Phys. Lett.* **1998**, *295*, 487. (b) Kato, H.; Kudo, A. *Catal. Lett.* **1999**, *58*, 153. (c) Kato, H.; Kudo, A. *J. Phys. Chem. B* **2001**, *105*, 4285. (d) Kato, H.; Asakura, K.; Kudo, A. *J. Am. Chem. Soc.* **2003**, *125*, 3082.
(21) Sato, J.; Kobayashi, H.; Saito, N.; Nishiyama, H.; Inoue, Y. *J. Photochem. Photobiol. A: Chem.* **2003**, *158*, 139.
(22) Sato, J.; Saito, N.; Nishiyama, H.; Inoue, Y. *J. Photochem. Photobiol. A: Chem.* **2002**, *148*, 85.
(23) Sato, J.; Kobayashi, H.; Ikarashi, K.; Saito, N.; Nishiyama, H.; Inoue, Y. *J. Phys. Chem. B* **2004**, *108*, 4369.
(24) (a) Dean, J. A. *Lange's Handbook of Chemistry*, 13th ed.; McGraw-Hill: New York, 1985. (b) Lide, D. R. *Handbook of Chemistry and Physics*, 83rd ed.; CRC Press: Boca Raton, FL, 2002.

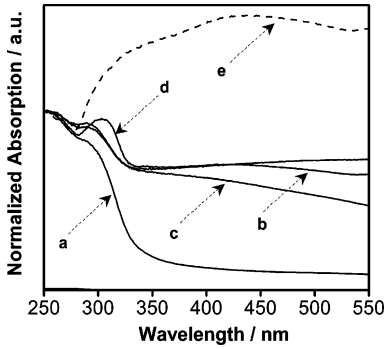

Figure 2. UV−vis diffuse reflectance spectra for samples obtained by nitriding GeO_2 under NH_3 flow for 10 h at (a) 1073, (b) 1123, (c) 1173, and (d) 1223 K. (e) Elemental Ge powder as a reference (High Purity Chemicals, Co.).

valence state of Ge^{4+} in addition to the formation process by which Ge_3N_4 is formed via elemental Ge. The nitridation capacity of NH_3 gas at 1073 K under the present experimental condition is likely to be too low to reduce GeO_2 to elemental Ge, although substitution of N^{3-} for O^{2-} anions proceeds weakly while maintaining the valence state of Ge^{4+} at lower temperatures.

UV−visible diffuse reflectance spectra for the same samples are shown in Figure 2 along with the data for Ge powder for reference. GeO_2, the starting material, does not exhibit any distinct absorption band in the wavelength range presented due to its high reflectance. All of the samples displayed two absorption bands: a sharp absorption peak in the UV region around 350 nm and a broad absorption peak extending into the visible region. The former is attributed to the band-gap transition of β-Ge_3N_4, which can be confirmed by photoexcitation−emission measurements as reported previously.[3a] The position of the absorption in the UV region did not undergo a significant shift regardless of nitridation temperature. Although a single phase of α-Ge_3N_4 could not be obtained under the present experimental conditions, it can be predicted by theoretical calculations that α- and β-Ge_3N_4 have similar band gaps.[25] Therefore, the absorption edges of the prepared samples are considered to be located close to 350 nm, despite the material being a mixture of α- and β-Ge_3N_4. On the other hand, the absorption in the visible region tended to increase with nitridation temperature from 1073 to 1123 K, primarily due to the appearance of the Ge phase (as indicated in the XRD pattern, Figure 1), which has a strong absorption coefficient in the visible region (spectrum e). The sample nitrided at 1173 K, exhibiting a single β-phase, also displayed an absorption in the visible region, although the intensity of the absorption was weaker than for the sample nitrided at 1123 K. The sample nitrided at 1173 K (i.e., β-Ge_3N_4) is brown in color, consistent with the report of Johnson.[7] Our previous study revealed that the visible-light absorption of β-Ge_3N_4 is due to defect sites and/or impurities, such as reduced Ge species.[3b] It is therefore considered that the sample nitrided at 1173 K contains impurities and/or defect sites even though it is a single phase of β-Ge_3N_4.

GeO_2 displayed no photocatalytic activity for overall water splitting even when loaded with RuO_2, primarily because it is soluble in aqueous media under ambient conditions[26] and has no spectral absorption. However, the nitrided materials exhibited simultaneous H_2 and O_2 evolution from pure water upon UV irradiation ($\lambda > 200$ nm). Figure 3 shows the time courses of water splitting for samples prepared by nitriding GeO_2 at various temperatures for 10 h with the RuO_2 modification. The photocatalytic activity of the sample can be seen to be dependent on the nitridation temperature of GeO_2. Although appreciable H_2 evolution was observed in all cases, the rates of O_2 evolution were more or less smaller than that expected from the stoichiometry. Furthermore, a relatively high level of N_2 evolution was observed in the reaction, indicating that the material is gradually decomposed by photogenerated holes. This decomposition consumes photogenerated holes that would otherwise be consumed in the oxidation of water as described by

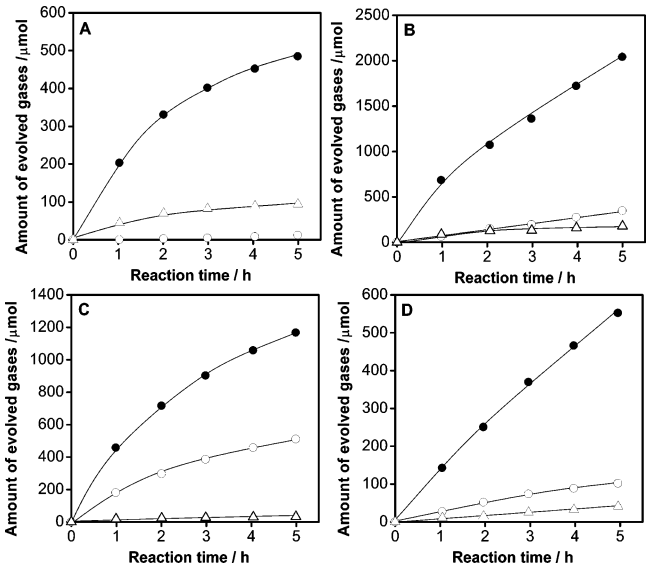

Figure 3. Time courses of overall water splitting under UV irradiation ($\lambda > 200$ nm) using samples obtained by nitriding GeO_2 under NH_3 flow for 10 h at (A) 1073, (B) 1123, (C) 1173, and (D) 1223 K. Reaction conditions: Catalyst, 0.3 g; distilled water, 360 mL; light source, high-pressure mercury lamp (450 W); quartz inner-irradiation-type reaction vessel. Solid circles, H_2; open circles, O_2; open triangles, N_2.

$$2N^{3-} + 6h^+ \rightarrow N_2 \quad (1)$$

However, as the nitridation temperature of GeO_2 increases (up to 1173 K), the rate of O_2 evolution approaches the stoichiometric value and N_2 evolution, indicative of the self-decomposition of the nitride photocatalyst, is increasingly suppressed. Nitridation at temperatures higher than 1173 K again results in deviation of the ratio of H_2 to O_2 from the stoichiometric value and is accompanied by the continuous evolution of N_2. As a result, the highest catalytic performance for overall water splitting was obtained in the present study for the sample nitrided at 1173 K. However, the rates of both H_2 and O_2 evolution over this material decreased with reaction time. As elucidated in the previous study, this degradation of activity is attributable to photoreduction of O_2, collapse of the catalyst surface by elution of Ge cations,

(25) Molina, B.; Sansores, L. E. *Int. J. Quantum Chem.* **2000**, *80*, 249.

(26) Linke, W. F. *Solubilities*, 4th ed.; D. Van Nostrand, Princeton, NJ, 1958; Vol. I. ((A-Ir) Inorganic and Metal-Organic Compounds).

Table 1. Total Gas Evolution after 5 h Reaction for Samples Prepared at Various Nitridation Temperatures

	total amount of evolved gases after 5 h of reaction[b]/μmol			
nitridation temp.[a]/K	H_2	O_2	N_2	*S* value[c]
1073	480	12	94	1.6
1123	2040	347	179	1.7
1173	1170	510	32	1.0
1223	550	102	41	1.7

[a] Nitridation for 10 h. [b] Data are taken from Figure 3. [c] Calculated by using eq 4. See text.

and degradation of the interfacial contact between Ge_3N_4 and the loaded RuO_2 nanoparticles.[3c]

Table 1 summarizes the total evolution of gases after 5 h of reaction for the various samples examined in this study (data are from Figure 3). Photocatalytic water reduction and oxidation reactions are expressed as follows.

$$2H^+ + 2e^- \rightarrow H_2 \quad (2)$$

$$2H_2O + 4h^+ \rightarrow O_2 + 4H^+ \quad (3)$$

On the basis of the eqs 1−3, the stoichiometry of the reaction products is evaluated by the relation

$$S = (\text{evolved } H_2)/\{(\text{evolved } O_2 \times 2) + (\text{evolved } N_2 \times 3)\} \quad (4)$$

When *S* is close to unity, the reduction (H_2) and oxidation (O_2 and N_2) products are well balanced, that is, stoichiometry is satisfied. As listed in Table 1, the *S* values for samples prepared at 1073, 1123, and 1223 K are larger than 1, while that for the sample nitrided at 1173 K is nearly equal to 1. The larger *S* value indicates excessive H_2 evolution, which in turn implies that some of the catalyst is oxidized by photogenerated holes and/or that other oxidation products such as peroxide species are generated during the reaction. It has been reported that excess H_2 evolution is sometimes observed during overall water splitting,[20a,20c,21,22] although the origin of this phenomenon has yet to be systematically clarified. In the present case all samples except for that prepared at 1173 K consist of a complex physical mixture containing either GeO_2, elemental Ge, or α- or β-Ge_3N_4 (Figure 1), precluding meaningful analysis of catalysts before and after reaction. Nevertheless, it should be noted that the stoichiometry of reaction products was satisfied when the single phase of β-Ge_3N_4 was used for the reaction.

3.2. Relationship between Structural Characteristics and Photocatalytic Activity of Ge_3N_4. On the basis of the results above it is speculated that the activity of Ge_3N_4 for the stoichiometric decomposition of pure water is dependent on the density of the β phase. Therefore, nitridation of Ge_3N_4 at 1173 K, which was found above to produce the single β phase after heating for 10 h, was conducted for a range of durations in order to obtain more insight into the relationship between the structural characteristics and photocatalytic activity of Ge_3N_4.

Figure 4 shows the XRD patterns of samples prepared by nitriding GeO_2 at 1173 K for several periods. The sample nitrided for 5 h contained β-Ge_3N_4 and a small fraction of α-Ge_3N_4. The diffraction peaks assigned to α-Ge_3N_4 disappeared upon nitridation for longer than 10 h after which a single phase of β-Ge_3N_4 was obtained. The diffraction peaks of β-Ge_3N_4 became stronger and narrower with increasing nitridation time from 5 to 15 h and then remained unchanged. These results indicate that crystallization of the nitridation product proceeds in the period from 5 to 15 h during nitridation at 1173 K accompanied by structural transformation of α-Ge_3N_4 into β-Ge_3N_4 between 5 and 10 h.

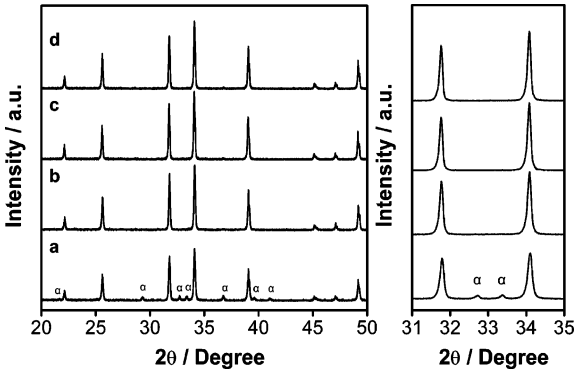

Figure 4. Powder XRD patterns of samples obtained by nitriding GeO_2 under NH_3 flow at 1173 K for (a) 5, (b) 10, (c) 15, and (d) 20 h. α denotes diffractions assigned to α-Ge_3N_4.

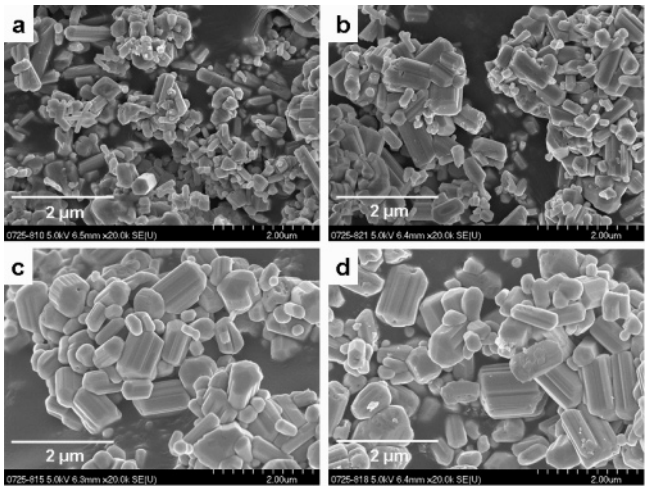

Figure 5. SEM images of samples obtained by nitriding GeO_2 under NH_3 flow at 1173 K for (a) 5, (b) 10, (c) 15, and (d) 20 h.

SEM images of these samples are shown in Figure 5. The sample prepared for 5 h consists of agglomerates of 200−400 nm diameter primary particles and rod-like particles ca. 1 μm in length. The particle size increased with nitridation time up to 15 h, beyond which the particle shape underwent no further change. This change in particle size agrees well with the XRD measurements. The specific surface area of these samples decreased gradually from 3.0 to 2.2 $m^2 \cdot g^{-1}$ with increasing nitridation time from 5 to 15 h, after which a constant value of 2.2 $m^2 \cdot g^{-1}$ was reached. This result is consistent with the SEM observation.

Figure 6 shows the UV−vis diffuse reflectance spectra for these samples. All samples produced a sharp absorption peak near 350 nm accompanied by a broad absorption in the visible-light region. The absorption near 350 nm, which originates from the band-gap transition of β-Ge_3N_4 from N 2p orbitals to hybridized Ge 4s,4p orbitals,[3a] did not change noticeably. On the other hand, the absorption band in the visible-light region, attributable to impurities and/or defect

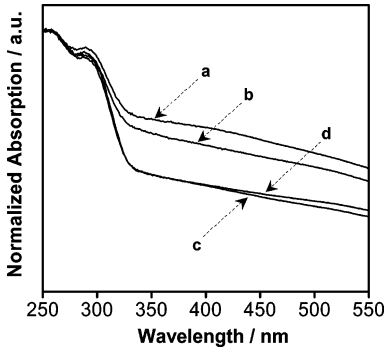

Figure 6. UV−vis diffuse reflectance spectra for samples obtained by nitriding GeO_2 under NH_3 flow at 1173 K for (a) 5, (b) 10, (c) 15, and (d) 20 h.

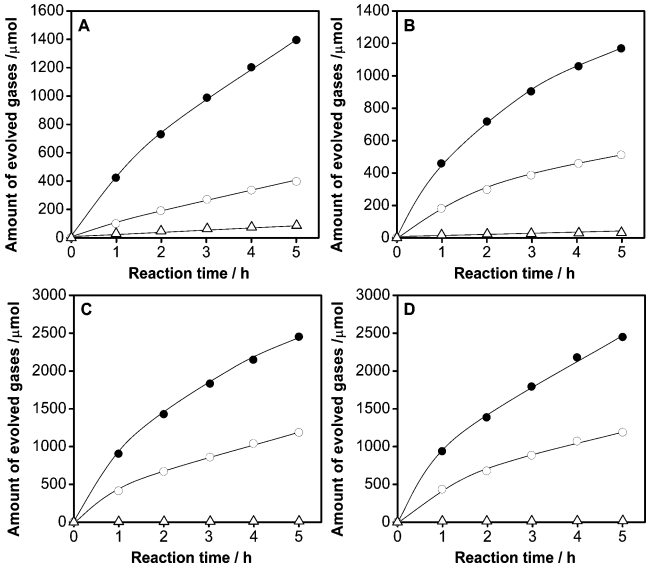

Figure 7. Time courses of overall water splitting under UV irradiation (λ > 200 nm) using samples obtained by nitriding GeO_2 under NH_3 flow at 1173 K for (A) 5, (B) 10, (C) 15, and (D) 20 h. Reaction conditions: Catalyst, 0.3 g; distilled water, 360 mL; light source, high-pressure mercury lamp (450 W); quartz inner-irradiation-type reaction vessel. Solid circles, H_2; open circles, O_2; open triangles, N_2.

sites,[3b] weakened with increasing nitridation time from 5 to 15 h, beyond which the spectrum remained almost unchanged. This result is similar to the previous result that high-pressure treatment of β-Ge_3N_4 under NH_3 gas reduces the density of defects and/or impurities, resulting in weakening of the visible-light absorption band.[3b] Therefore, extended annealing under NH_3 flow is also effective for reducing the density of defect sites and/or impurity phases.

Figure 7 shows the time courses of water splitting over these Ge_3N_4 catalysts when loaded with 1 wt % RuO_2. Simultaneous H_2 and O_2 evolution was achieved for all catalysts regardless of nitridation time. With increasing nitridation time, however, the rates of H_2 and O_2 evolution approached the stoichiometric ratio, reaching a maximum for samples nitrided for 15 h or longer. The catalysts nitrided for 15 h or longer thus provided the best photocatalytic performance observed in this study, and the total H_2 and O_2 evolution over 5 h of reaction (3.6 mmol) was substantially greater than the amount of catalyst employed (0.3 g; 1.1 mmol of β-Ge_3N_4), confirming the catalytic cycle. The enhanced activity of RuO_2-loaded Ge_3N_4 with increasing nitridation time is primarily associated with the improvement in the crystallization of the material. In the nitridation period between 5 and 15 h, where the largest increase in activity was obtained, the XRD peak became stronger and narrower (Figure 4) and the particles of Ge_3N_4 grew significantly (Figure 5) with an accompanying decrease in the density of defects and structural imperfections that can act as recombination centers between photogenerated electrons and holes. This decreasing concentration of defect sites in Ge_3N_4 is also supported by the change in the visible-light absorption band in the diffuse reflectance spectrum (Figure 6). Such correlation between the activity and the degree of crystallization is a general trend recognized for other photocatalysts, in particular, metal oxides.[18c,21,23] Although it has been reported that prolonged and/or high-temperature calcination of metal-oxide photocatalysts can result in reduced activity, due primarily to a reduction in specific surface area,[18c,21,23] it appears that longer nitridation of Ge_3N_4 has no detrimental effect on activity. This is probably because the specific surface area does not change noticeably upon further nitridation, as mentioned above.

It is known that polymorphs of a given metal oxide display unique photocatalytic activity.[27,28] In the case of overall water splitting, Abe et al. reported that metal oxides expressed by R_3MO_7 and $R_2Ti_2O_7$ (R = Y, Gd, La; M = Nb, Ta), having different crystal structures, exhibit different photocatalytic activities.[28] Unfortunately, however, the individual activity of α- and β-Ge_3N_4 for overall water splitting cannot be compared on a similar basis since α-Ge_3N_4 is a metastable phase and thus difficult to prepare as a single phase, at least under the present experimental conditions. Nevertheless, on the basis of the above results it can be concluded that the photocatalytic activity of Ge_3N_4 for overall water splitting is dependent on the generation of well-crystallized β-phase with minimized defect density.

The quantum efficiency for the photocatalytic reaction, which is a more reliable measure of activity than the rate of gas evolution under a given reaction condition, could not be measured reliably for RuO_2-loaded β-Ge_3N_4 due to photoreduction of O_2, a backward reaction of overall water splitting that proceeds strongly in this reaction.[3c] When the quantum efficiency is measured using an external-irradiation-type reaction vessel with a monochromator or xenon lamp, the number of gas molecules produced in the reaction becomes inevitably small due to the lower intensity of incident light and hence the number of incident photons. In such a situation the probability that evolved O_2 is reduced by the photogenerated electrons in the conduction band of β-Ge_3N_4 before leaving the β-Ge_3N_4 surface increases, causing the apparent reaction rate measured by gas chromatography to be lower.

For non-oxide photocatalysts, it is important to discuss the effect of self-decomposition by photogenerated holes in the valence band of the material since this process competes with the water photooxidation reaction. Figure 8 shows the time courses of N_2 evolution for overall water splitting over

(27) (a) Sclafani, A.; Herrmann, J. M. *J. Phys. Chem.* **1996**, *100*, 13655. (b) Abe, R.; Sayama, K.; Sugihara, H. *J. Phys. Chem. B* **2005**, *109*, 16052.
(28) Abe, R.; Higashi, M.; Sayama, K.; Abe, Y.; Sugihara, H. *J. Phys. Chem. B* **2006**, *110*, 2219.

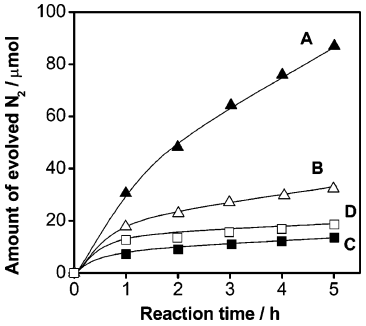

Figure 8. Time courses of N_2 evolution in overall water splitting under UV irradiation (λ > 200 nm) using samples obtained by nitriding GeO_2 under NH_3 flow at 1173 K for (A) 5, (B) 10, (C) 15, and (D) 20 h. Reaction conditions: Catalyst, 0.3 g; distilled water, 360 mL; light source, high-pressure mercury lamp (450 W); quartz inner-irradiation-type reaction vessel.

Scheme 1. Photooxidation of H_2O into O_2 (Process 1) and N^{3-} into N_2 (Process 2) Near the Surface of β-Ge_3N_4

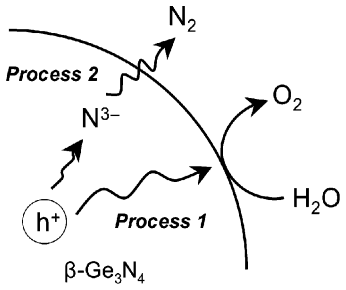

RuO_2-loaded Ge_3N_4 catalysts prepared by nitridation for a range of periods (data are from Figure 7). The catalyst nitrided for 5 h released N_2 continuously as the reaction progressed, indicating that self-decomposition took place according to eq 1. However, with increasing nitridation time N_2 release from the catalyst suspension was suppressed considerably. The observed N_2 evolution during the reaction occurs near the catalyst surface,[29] while O_2 evolution takes place catalytically directly on the Ge_3N_4 surface. Therefore, photogenerated holes to be consumed in O_2 evolution must migrate over a longer distance compared to those involved in N_2 evolution, as illustrated in Scheme 1. As the crystallinity of Ge_3N_4 improves, the photogenerated electrons and holes can more readily migrate longer distances, resulting in a higher likelihood that the electrons and holes will reach the surface reaction sites without recombining. The present experimental results are thus considered reasonable since the rate of O_2 evolution increases with the crystallinity of Ge_3N_4 while the rate of N_2 evolution decreases. Our group has previously reported that a decrease in the pH of the reactant solution suppresses N_2 evolution in overall water splitting using RuO_2-loaded β-Ge_3N_4 by inhibiting hydrolysis-induced deactivation in neutral or basic media, leading to enhanced activity.[3c] In addition to such a kinetic control, N_2 evolution can be effectively suppressed by improving the crystallinity of β-Ge_3N_4. It was also found that when the reaction is repeated after evacuation of gas phase, the β-Ge_3N_4 catalyst that had undergone surface oxidation due to a release of N_2 exhibits slightly lower activity than that being less oxidized. In metal-oxide photocatalysts, high crystallinity has a positive effect on the rates of H_2 and O_2 evolution in overall water splitting since the density of defects, which frequently act as recombination centers between photogenerated carriers, decreases with increasing crystallinity.[18c,21,23] In metal-nitride photocatalysts, however, high crystallinity is a crucially important factor affecting the stability of the material in addition to promoting H_2 and O_2 evolution in overall water splitting.

(29) Maeda, K.; Teramura, K.; Masuda, H.; Takata, T.; Saito, N.; Inoue, Y.; Domen, K. *J. Phys. Chem. B* **2006**, *110*, 13107.

4. Conclusion

β-Ge_3N_4 was successfully prepared by nitriding GeO_2 at 1173 K for longer than 10 h and demonstrated to be photocatalytically active for the stoichiometric decomposition of pure water. The activity of RuO_2-loaded Ge_3N_4 for this reaction was shown to be dependent on the crystallinity and density of defects in the material. As the crystallinity of β-Ge_3N_4 increases, self-decomposition of the material (i.e., N_2 release) by photogenerated holes is suppressed, contributing to improved efficiency of overall water splitting.

Acknowledgment. This work was supported by the Core Research for Evolutional Science and Technology (CREST) and Solution Oriented Research for Science and Technology (SORST) programs of the Japan Science and Technology Corporation (JST). Acknowledgment is also extended to the 21st Century Center of Excellence (COE) and the Research and Development in a New Interdisciplinary Field Based on Nanotechnology and Materials Science programs of the Ministry of Education, Science, Sports and Culture (MEXT) of Japan. K.M. gratefully acknowledges the Japan Society for the Promotion of Science (JSPS) Fellowship.

CM0709828